Considerations of Application Examples of Gait Analysis Using MediaPipe

Yasutaka Uchida
Dept. of Life Science
Teikyo University of Science
Tokyo, Japan
e-mail: uchida@ntu.ac.jp

Tomoko Funayama
Dept. of Occupational Therapy
Teikyo University of Science
Yamanashi, Japan
e-mail: funayama@ntu.ac.jp

Eiichi Ohkubo
Dept. of Life Science
Teikyo University of Science
Tokyo, Japan
e-mail: ohkubo@ntu.ac.jp

Yoshiaki Kogure
Professor Emeritus
Teikyo University of Science
Tokyo, Japan
e-mail: kogure@ntu.ac.jp

Yasunori Fujimori
Dept. of Rehabilitation
Seirei Yokohama Hospital
yasu6622@outlook.jp

Ryota Kimura
Dept. of Rehabilitation
Seirei Yokohama Hospital
ryota151@infoseek.jp

Kohei Kimura
Dept. of Rehabilitation
Seirei Yokohama Hospital
13rp13@g.seirei.ac.jp

Abstract— **MediaPipe, which enables skeletal analysis utilizing videos of walking subjects without markers, can be easily introduced into rehabilitation sites. The viewpoint is obtained from a single camera because the video utilized for analysis is captured from a smartphone or video camera. Therefore, the skeletal coordinates cannot be recognized during analysis, and the obtained coordinates are relative values. Here, we employed data obtained from MediaPipe to calculate stride length, walking speed, knee height change, and ankle angle and compared them with commercially available software. A pseudo-motor restriction was applied during the measurements by wearing a supporter on the right knee. We found that the presence of motion restriction and various parameters during gait can be obtained by combining the confirmation of gait trajectory with 3D analysis and clarifying the measurement range. In addition, patients undergoing rehabilitation were asked to wear walking aids, and the walking patterns before, during, and after wearing them were analyzed with MediaPipe to confirm the effectiveness of the walking-assisted aid attachment.**

Keywords- MediaPipe; skeletal analysis; smartphone; 3D analysis; walking-assisted aid attachment; spectrometry.

I. INTRODUCTION

Measures are urgently required to prepare for a rapidly aging population. Falling is a significant problem among older people, as it causes them to be bedridden and places a heavy burden on their caregivers [1]-[8]. Therefore, motion analyses have been conducted utilizing insoles [9]-[11] and mat-like pressure sensors arranged two-dimensionally [12][13], wearable devices [14][15], and images [16][17]. For gait analysis, measurements utilizing multiple cameras with attached markers have been utilized in rehabilitation facilities, as represented by the Vicon system [18][19]. A camera called Kinect [20][22] has also been utilized to analyze the movement of a camera [22][23] linked to game software. However, problems remain, such as the need for an expensive dedicated system, space for recognizing the markers, and an operator familiar with the dedicated software. The rapid spread of smartphones has facilitated the capturing of pictures anytime and anywhere, and the threshold for capturing pictures has decreased. Moreover, excellent paid and easy-to-utilize software is available. However, introducing a system requires continuous expenditure, which is currently in a state where it cannot be sufficiently spread.

Software that can perform skeleton authentication includes OpenPose [24][25], developed by Carnegie Mellon University, and MediaPipe [26]-[30], released by Google. Both apply deep learning and have an advanced certification system.

At Global Health 2022, we presented a basic application of MediaPipe in rehabilitation. Furthermore, for the utilization of a walking-assist device, we reported that the effect continued approximately 5 min after the device was removed. This paper reports additional research results on the accuracy and application range of walking parameters obtained utilizing MediaPipe. If the analysis results from front filming can be utilized, data captured in hallways can also be utilized. Here, we performed the analysis utilizing front filming. MediaPipe, which can utilize Python, can be used by healthcare and welfare professionals who are not analysis experts. The ability to analyze videos from the front view via MediaPipe can also enable filming in rehabilitation rooms and hallways of hospitals and facilities; thus, healthcare and welfare professionals can utilize it themselves. This paper reports additional analysis results regarding the accuracy and applicability of parameters obtained from MediaPipe during walking and the results of walking analysis conducted on a participant who had atherothrombotic cerebral infarction.

Section II describes the experimental methodology, including the software utilized and the commercially available equipment and software. In Section III, we compare the results of measurements conducted on healthy individuals utilizing MediaPipe and commercially available software with the analysis results obtained utilizing MediaPipe during rehabilitation sessions for participants with atherothrombotic cerebral infarction. Section IV discusses the results obtained from the two types of software and the measurement results of individuals during rehabilitation, comparing the assessments from therapists with the results obtained from MediaPipe. Section V presents the conclusions.

II. EXPERIMENTS

We developed a method for analyzing MediaPipe data using a male in his 60s, represented by subject A, and validated it with a male in his 70s, represented by subject B, in rehabilitation training.

A. Establishment of Analysis Method

The participant was a male in his 60s. During the measurement, his right knee was fixed with a supporter to pseudo-restrict his movement, and a comparison was made utilizing the tool ORPHE ANALYTICS ® [31] to confirm the accuracy of the calculation results obtained from the 3D coordinate data obtained via MediaPipe. This software enabled us to attach ORPHE CORE®, which utilizes acceleration and angular rate meters, to the instep of a shoe using a special attachment that can be fixed to the shoelace. The data obtained from these sensors could be analyzed to display various results. A photograph of the ORPHE CORE® attached to the shoelaces is presented in Figure 1.

Figure 1. ORPHE CORE® attached to shoelaces using an attachment.

Owing to the limitations of the laboratory, we could not utilize the timed up-and-go method, in which the participant stands from a seated position in a chair, walks around a cone 3 m away, and sits down again while being observed and photographed from the lateral direction. Therefore, to enable analysis utilizing ORPHE ANALYTICS from the front, we utilized an iPhone with ORPHE TRACK installed to receive acceleration signals from ORPHE CORE via Bluetooth; simultaneously, the data of the walking state were uploaded to the cloud service.

A video of the walking condition displayed on the ORPHE ANALYTICS screen was recorded at 720p utilizing the free AG Desktop Recorder software. This screen was loaded into MediaPipe and operated using Jupyter Notebook in Python to obtain 3D data corresponding to 33 locations on the Land Marker. From these data, we extracted data for the left and right hips, knees, ankles, and toes. Based on these data, Python displayed the trajectories of the knees and other parts of the body in 3D. In addition, Microsoft Excel was employed to calculate the change in the difference between the knee and ankle. The ankle angle was calculated with vectors connecting the ankle and knee and the ankle and toe.

Figure 2 presents examples of measurements utilizing MediaPipe. The image on the left depicts measurement without motion restriction, and the image on the right depicts that with motion restriction as indicated by the yellow circle.

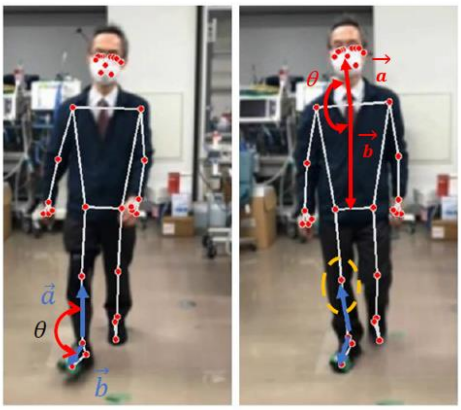

Figure 2. Examples of measurement results.

The supporter restricting movement is worn on the right knee, although it is difficult to see from the photo.

B. Gait Training Measurement

Gait was measured in subjects who are hospitalized and receiving training in physical therapy (PT) and occupational therapy (OT). The participant who underwent measurements at the hospital is a single individual with the following specific characteristics: a male in his 70s, right-handed. His diagnosis was atherothrombotic cerebral infarction (right putamen, corona radiata, subcortical parietal lobe); his disabilities were left hemiplegia, dysarthria, attention disorder, and left hemispatial neglect; his medical history included cerebral contusion, hypertension, and a left femoral neck fracture. Before the stroke, he was independent in his daily activities and occasionally went shopping at a local supermarket. Rehabilitation comprising PT, OT, and speech and hearing therapy commenced the day following the stroke. PT consisted of gait training five times a week for 40 min each. Sixteen days after the stroke, a gait evaluation utilizing a robot was conducted. Owing to the history of cerebral contusion, it is possible that the decline in motor function is not limited to the left side of the body but may also be present on the right side.

Figure 3 presents a photograph of the Orthobot® equipped for walking-assisted attachment.

Figure 3. Photograph of walking with walking-assisted aid attachment.

In this paper, we refer to the subject of the analysis method as subject A and the subject of the gait training as subject B.

This study was approved by the Ethics Committee on Research with Humans as Subjects of the Teikyo University of Science. This experiment was conducted in accordance with the Declaration of Helsinki.

III. EXPERIMENTAL RESULTS

A. Analysis Method

A-1. Measurement of Strides

The right-foot ankle trajectory of subject A measured with the MediaPipe is illustrated in Figure 4. Only one round trip was utilized in the analysis. This is because plotting the trajectory of a round-trip walking state would cause the trajectories to cross each other, making them difficult to read. Because the camera is fixed, the coordinate data are x and y values corresponding to the 2D screen, except for the z-axis coordinates in the depth direction, which are relative, a characteristic of MediaPipe. Therefore, the data for one round trip were adopted here because performing a simple analysis is difficult. The amplitude increased until the change of direction occurred, indicating that the z-axis value did not change significantly during the change in direction. The area from the start of the walk to the change in direction was obtained.

The z-axis values for walking when approaching the camera are presented in Figure 5.

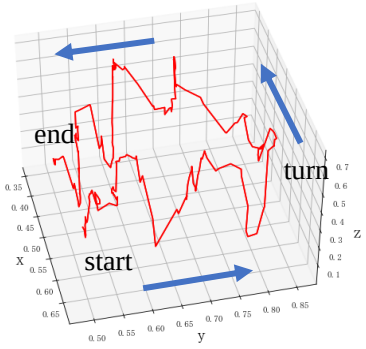

Figure 4. Right-foot ankle trajectory measured with MediaPipe.

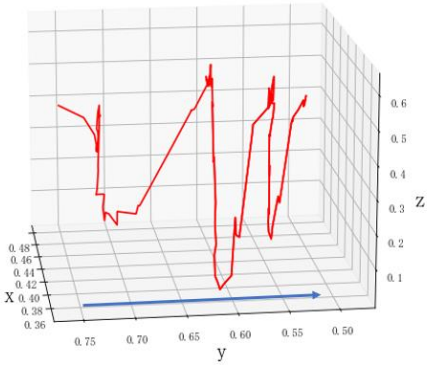

Figure 5. Z-axis values for walking when approaching camera.

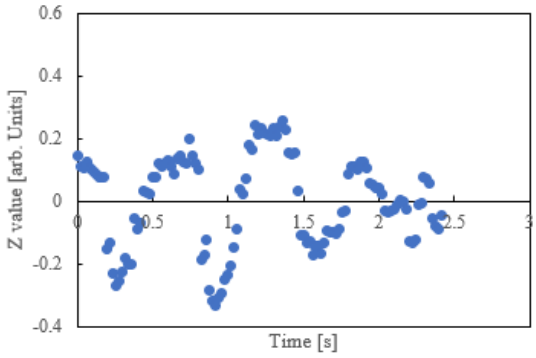

Figure 6. Result of modifying effect of walking direction.

Numerical data were displayed in Excel, and the inclination due to the walking direction was obtained; the corrected results are presented in Figure 6. Utilizing this diagram, we considered the point corresponding to the landing to be the minimum value based on the change in amplitude. As the figure demonstrates, the amplitude increased as the participant approached the camera, and the center of the amplitude also increased. Therefore, the center of the amplitude was approximated as increasing with a linear function, and the difference from the coordinate data was considered. The minimum value was set as the foot's landing point when the amplitude varied periodically, although a certain variation was observed. The actual measurement was obtained from the screen position, and the stride length was determined as the distance between the landing points. Walking speed was calculated from the respective times.

In the MediaPipe, the stride length was 0.80–0.90 m, and the velocity obtained was 0.8 m/s. The stride lengths of the left and right legs were 0.70 and 0.80 m, respectively. The stride length was larger in the right leg, with restricted motion owing to the hip motion.

The left and right stride lengths obtained from ORPHE were 0.75 and 1.0 m, respectively, larger than the values obtained from MediaPipe. In both cases, the value for the right leg was larger. The walking speeds on the left and right sides were 0.78 and 0.76 m/s, respectively, which were almost the same.

A-2. Calculation of Knee Height

Figure 7 presents the results of the changes in the right and left knee heights using MediaPipe during the gait of subject A. Red indicates the right knee with limitation of motion by the supporter, and blue indicates the left knee without limitation of motion. Here, the results are also presented from the beginning of walking to turning, considering the effect of rotation.

The results of the ORPHE ANALYTICS measurement of knee height are presented in Figure 8. The upper-left corner of the screen is the origin, and the maximum y-axis corresponding to the vertical direction is represented by 352 pixels. Therefore, the height of the right knee, which is a small

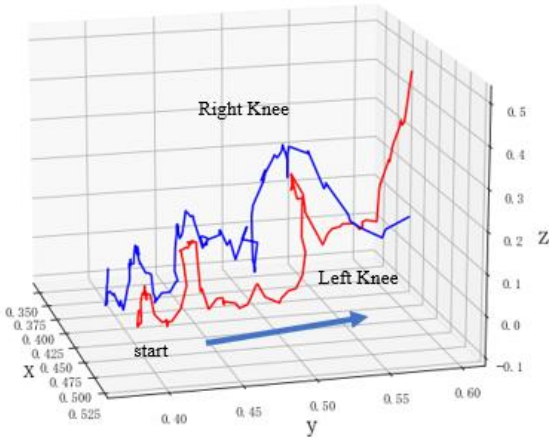

Figure 7. Height of knee position evaluated with MediaPipe.

value in the figure, had a higher value. The horizontal axis represents the number of measurement points for data analysis and not the time axis. The y-axis value for the x-axis, which corresponds to the direction of motion, changed significantly when the participant changed the gait direction during the measurement. When comparing knee heights, we utilized moving images and changes in the x-axis direction, which is characteristic of a change in direction. We deleted data from points in the range that appeared to indicate a change in the turn direction.

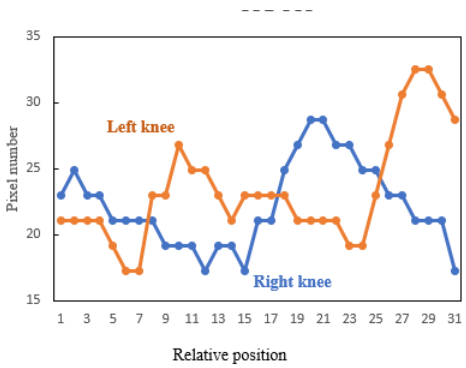

Figure 8. Knee height measurements with ORPHE ANALYTICS.

B. *Feature Extraction of Gait Training Effect*

B-1. Measurement Results of Blurring of Nasal Trajectory

We examined the instability of subject B undergoing rehabilitation while walking by analyzing the trajectory of the nose region. The assistant from behind is supporting the upper arm to prevent falls. Measurements were taken before, during, and after walking-assisted aid attachment. The image was captured from the front because of facility constraints. While shooting from the arrow direction is preferred, we considered the extent of assessment possible from the front image this time. The participant is wearing a mask, but MediaPipe recognizes the nose.

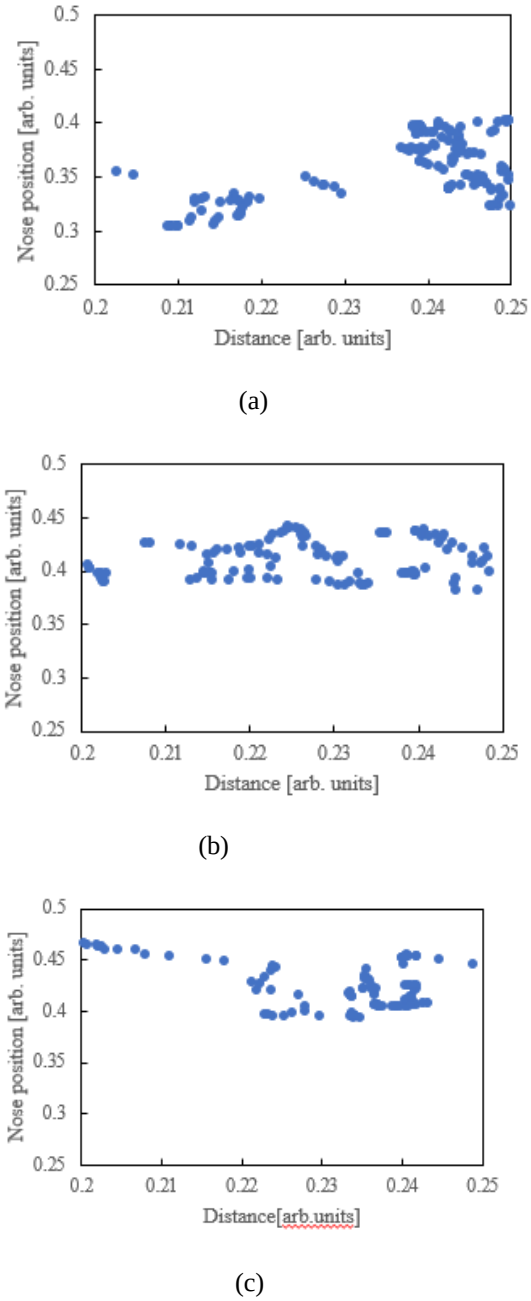

Figure 9. Blurring of nasal trajectory

Figure 9 illustrates the trajectory of the nose coordinates with respect to the walking direction. Because the walking direction is given as a relative value in MediaPipe, the same walking section was plotted for comparison. In the figure, (a) is before utilizing walking-assisted aid attachment, (b) is while utilizing walking-assisted aid attachment, and (c) is after utilizing walking-assisted aid attachment.

B-2. Measurement Results of Shoulder Tilt While Walking

Figure 10 (a) represents the subject B's results before utilizing the walking-assisted aid, (b) while utilizing the walking-assisted aid, and (c) after utilizing the walking-assisted aid. The changes in shoulder inclination during walking were determined based on the left shoulder.

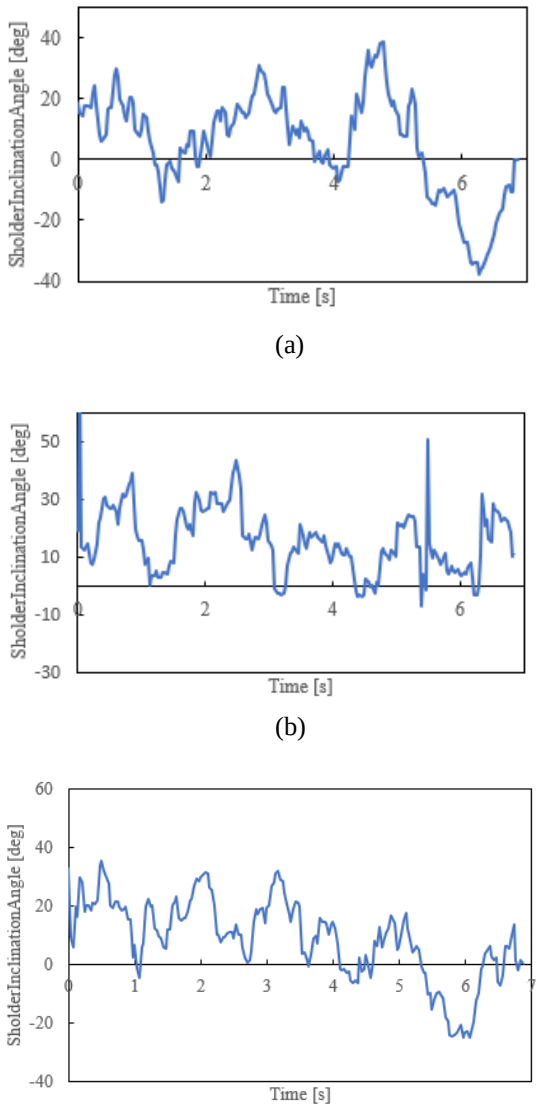

Figure 10. Shoulder tilt while walking.

B-3. Measurement Results of Hip Tilt While Walking

Figure 11 (a) represents the subject B's results before using the walking-assisted aid attachment, (b) while using the walking-assisted aid attachment, and (c) after using the walking-assisted aid attachment. The changes in hip inclination during walking were determined based on the left hip.

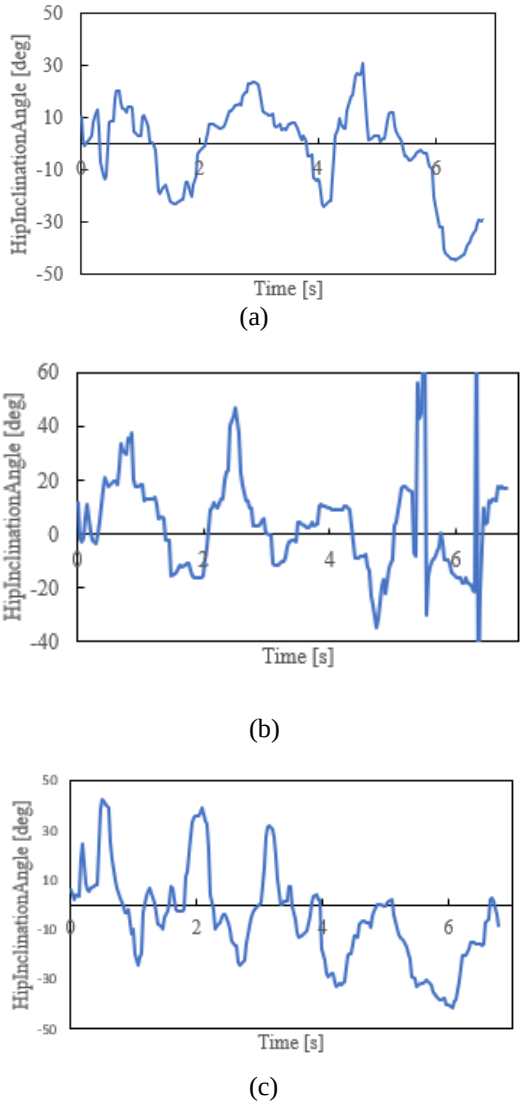

Figure 11. Hip tilt while walking.

The inclinations of the shoulder and hips demonstrated almost the same tendency.

B-4. Measurement Results of Neck Tilt While Walking

Walking affects not only the lower limbs but the whole body. This section focused on the head and neck parts of the body. An inverted pendulum model was utilized for walking. Based on the coordinate information obtained from MediaPipe, we calculated how much the subject B's neck tilts from the central axis of the torso when walking. Figure 2 depicts the line connecting the coordinates of the midpoint of the left and right shoulders with the coordinates of the midpoint of the left and right hips, and the line connecting the coordinates of the midpoint of the left and right hips with the left and right shoulders and the tip of the nose. The angle formed was defined as the neck angle, calculated with the formula for interior angles of vectors. The results are presented in Figure 12.

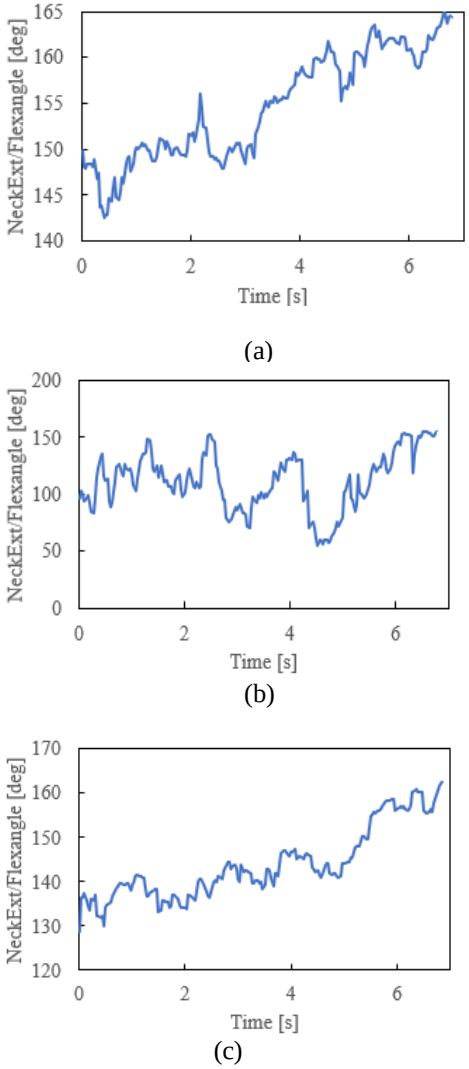

Figure 12. Neck angle while walking.

Because the vibration of the head tilt is considered to be different depending on each condition, the results of obtaining the discrete Fourier transform (DFT) spectrum are presented in Figure 13. The spectrum above 2 Hz becomes stronger after utilizing the walking aid attachment.

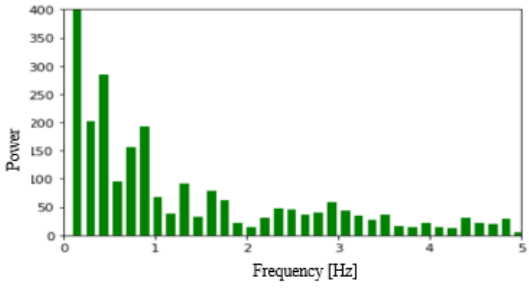

(a)

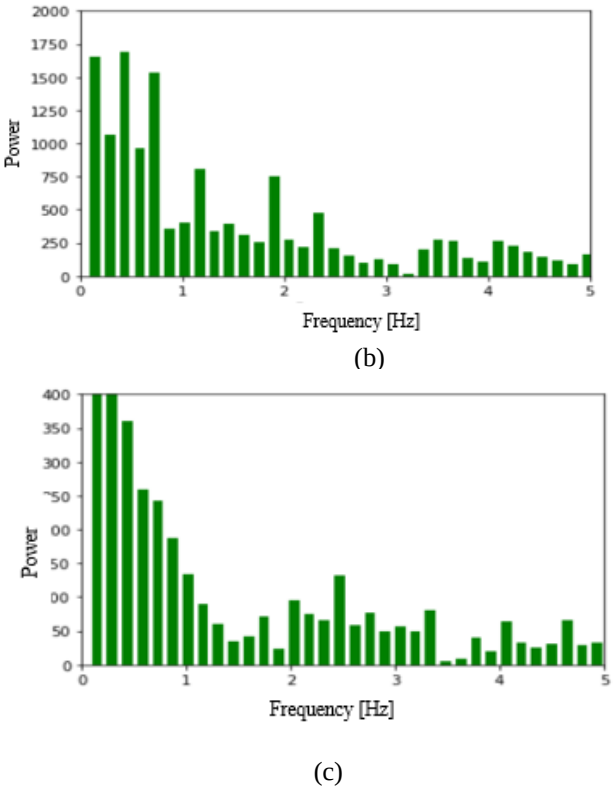

Figure 13. Neck DFT spectra.

B-5. Measurement Results of Foot DTF Spectrum While Walking

DFT spectrum analysis of left foot was performed because it was observed that the left and right legs moved periodically during the subject B walking when wearing a walking aid attachment. The results are presented in Figure 14, where (a) represents the left foot, (b) is while utilizing the walking aid, and (c) is after.

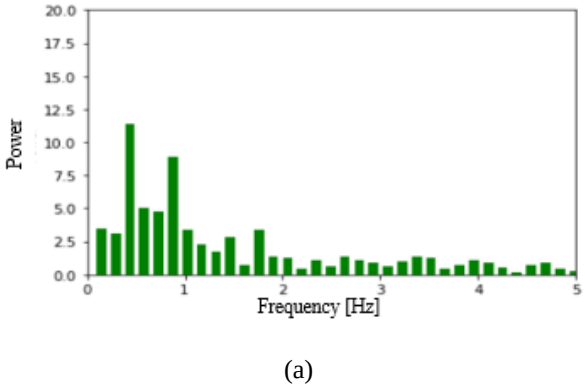

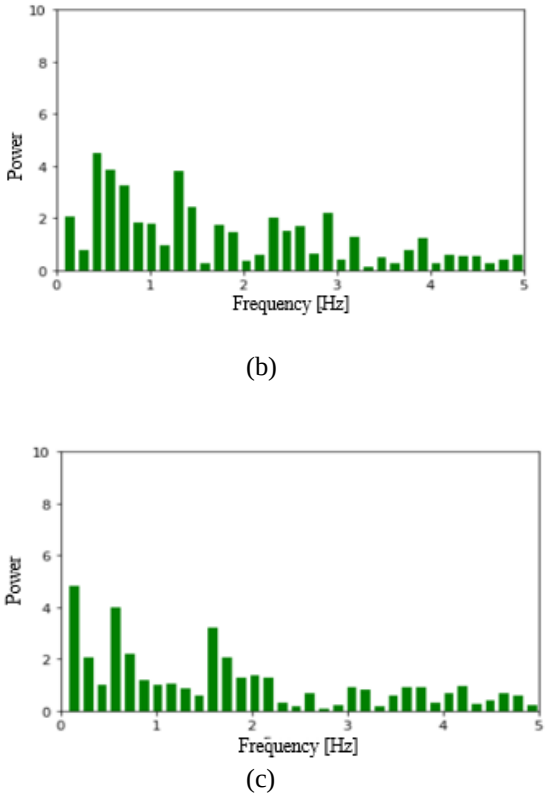

Figure 14. Foot DFT spectra.

The spectrum above 1.6 Hz becomes stronger after utilizing the walking aid attachment.

B-6. Determination of Rhythmic Heel Change by Time Series

Figure 15 illustrates the results of calculating a spectrogram [32] to clarify the frequency spectrum of left and right heel wobbling before and after wearing a walking aid attachment. (a) and (b) are the left and right heels before wearing them, and (c) and (d) are the left and right heels after removing the attached assisted device.

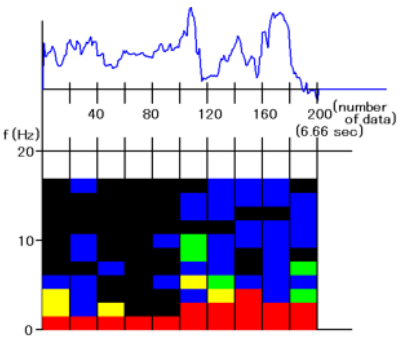

(a) Left heel.

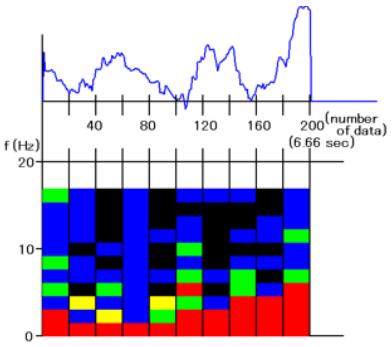

(b) Right heel.

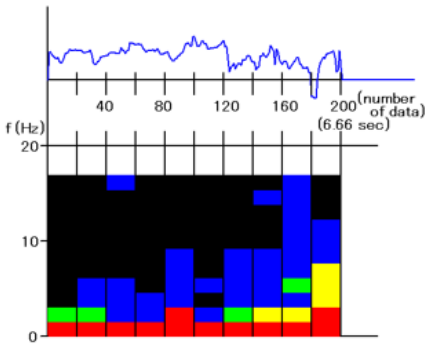

(c) Left heel.

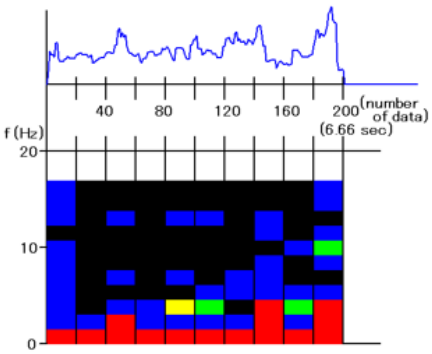

(d) Right heel.

Figure 15. Spectrogram of heel position vibration

B-7. Stride and Gait Speed measurement results

The minimum points of the heel position in Figure16 (a) to 16 (c) are considered as the ground contact point. Furthermore, a ruler was placed separately in the walking area to visually determine the heel position, and the relationship between walking step and heel position is illustrated in Figure 17. In this figure, (a), (b), and (c) respectively represent before utilizing the walking aid, during utilization, and after.

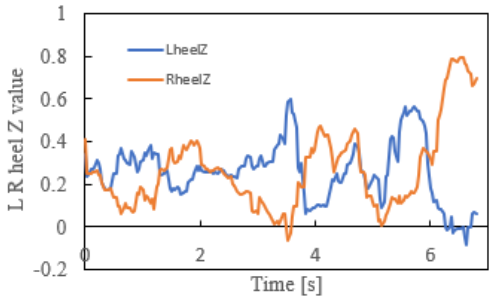

(a)

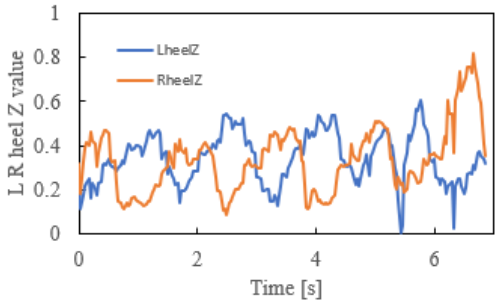

(b)

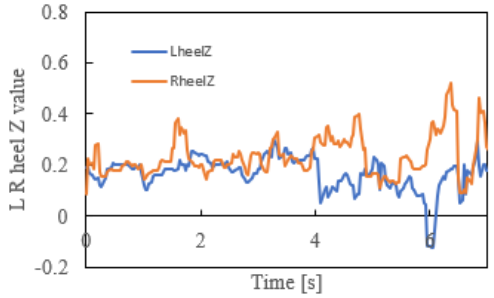

(c)

Figure 16. Positions of heels.

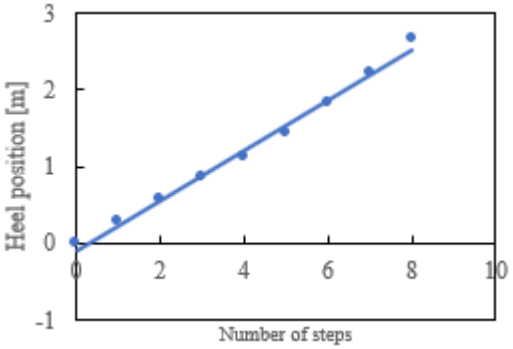

(a)

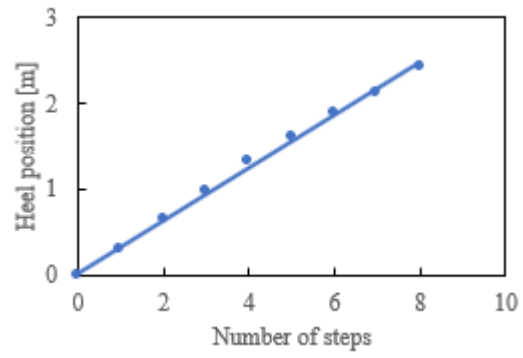

(b)

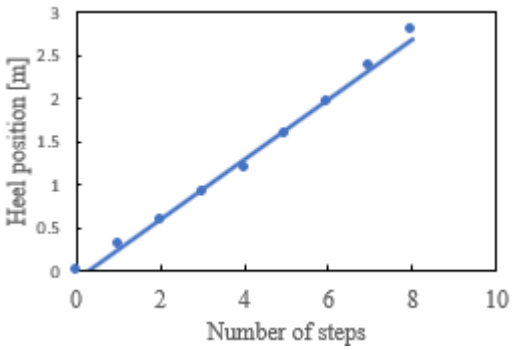

(c)

Figure 17. Heel position as function of steps.

Comparing the three figures, it is observed that the stride length improved before, during, and after utilizing the walking aid attachment.

IV. DISCUSSION

A. *Differences in Measurement Results Based on Coordinate Axes Derived from Measurements in Subjects without Gait Disorders*

In this experiment, the main reason for the difficulty in the analysis was that the measurement had to be performed under conditions where frequent changes in direction occurred owing to the limitations of the measurement location. Because the left and right foot coordinate values were different owing to the camera angle, simple comparison and analysis were impossible; a combination of 3D plots is considered necessary for motion analysis of the knee and ankle. In contrast, ORPHE ANALYTICS®, a commercially available software, provided data with correction. However, although it provided sufficient characteristic data of gait in terms of coordinate values, it was more difficult to handle than MediaPipe owing to the limited number of pixels; therefore, it may not have provided sufficient accuracy.

The data were limited to a specific individual because there was only one participant in this measurement. It would be necessary to increase the number of participants in the future. In addition, an accurate evaluation can be conducted by changing the fixation position of the ORPHE CORE® to the inside of the shoe for measurement and comparison.

B. *Consistency with Gait Assessment by Physical and Occupational Therapists and MediaPipe Results*

B-1. Blurring of Nasal Trajectory

To evaluate the shaking while walking, we judged the state of the nose, the center of the left and right shoulders, etc., from images, and the PT and OT pointed out that the movement of the nose was the most noticeable. Table I presents the standard deviation of nasal part blur for each walking condition.

Table 1. Standard deviation of nasal part blur for each case

Before assisted aid attachment	During assisted aid attachment	After assisted aid attachment
2.90E-02	4.30E-04	1.40E-04

As presented in the table, the value was lowest when utilizing walking aids and remained low even after utilizing walking aids. This suggests that the effect of the walking aid continues for some time, even in persons with hemiplegia. The effect continued even after utilization, which was the same as in the case of healthy participants reported last year.

B-2. Shoulder Tilt While Walking

The PT and OT observation resulted in an assessment indicating that the right shoulder remained elevated regardless of the utilization of walking aids. The inclination derived from the coordinates of MediaPipe revealed an instantaneous state where the right shoulder dropped compared to the left shoulder within approximately 5 s from the start of walking. The photographs of these points are presented in Figure 18. However, beyond 5 s, data depicting the right shoulder dropping and abrupt peaks were observed. The instantaneous peaks were recognized as corresponding to the right shoulder dropping in relation to the landmark corresponding to the shoulder in MediaPipe.

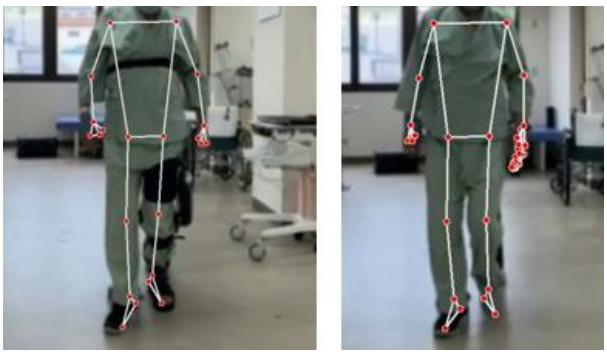

Figure 18. Photographs of right shoulder dropping.

It was decided to calculate and compare the area ratios to examine the discrepancies with the assessment. Because the data from MediaPipe were obtained at regular intervals, calculating the area by integrating the shoulder inclination angles over time was believed to enable a more accurate comparison. The area was determined by integrating the tilt angle up to 6.8 s, which is the same time for all measurements. Based on before walking-assisted aid attachment, the ratio was 1.0:4.0:3.3. The left side is decreasing because the area becomes a positive value in all cases when integrated. Based on the opinions from PT and OT, we reconsidered that the data before and during the utilization of the walking aid on the screen were calculated to be small. The results are greatly affected by the fact that the integrated area is small because the swing is large in the negative direction at a distance close to the camera. When we examined the video being analyzed in MediaPipe in detail, we found that after 5 s, it became clear that there was a possibility that the points of the marks were not sufficiently recognized. Based on this result, the area integrated over the 5 s before the sudden change was the smallest when utilizing a walking aid attachment.

B-3. Hip Tilt While Walking

Observation of the PT and OT revealed that the left hip joint was located lower than the right hip because the center of gravity shifted outward during the stance phase when the right lower limb was bearing the weight. Therefore, the position of the right hip joint is higher than that of the left hip joint. After walking-assisted aid attachment treatment, the body's weight-bearing ability when the hip joint extends during the late left stance has improved. Hence, it is now possible to bear weight during the early right stance, reducing lateral bending of the left trunk. The assessment was that the hip joint position was relatively higher on the right than on the left. The observation is correlated with the evaluation from Figure 11, which assessed the inclination of the hip based on the MediaPipe data, noting that the top amplitude is relatively small. During the utilization of walking-assisted aid, support is achieved during the left hip extension, equivalent to the stance phase late in the gait cycle. Hence, a significant amplitude is observed in the hip joint movement. This effect persists even in the lowermost part of Figure 11 after utilizing walking-assisted aid, indicating that the impact continues over time.

Figure 19 is a photograph comparing the degree of heel rise. The image illustrates the state of walking when the walking aid device is removed.

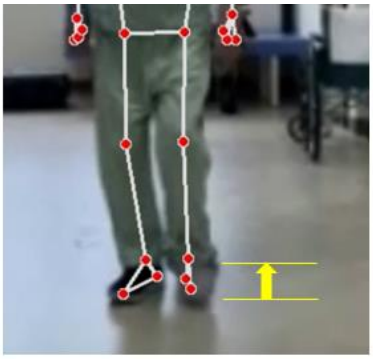

Figure 19. Photograph comparing heel height.

To determine whether the therapist's idea of improved weight bearing capacity in the late left stance phase could be judged by the heel rise, that is, the change in the final time of kicking the floor, we calculated the heel height with MediaPipe. However, it was impossible to determine that the heel position was higher after utilizing the robot than before. No evidence was found to support the therapist's consideration.

C. Neck Tilt While Walking

In measurements of a healthy individual last year, the utilization of walking aids resulted in a strong low-frequency signal spectrum below 0.5 Hz regarding the vertical oscillation of the neck during walking. However, in the case of the participant undergoing rehabilitation, spectra below 0.5 Hz in the low-frequency region were also observed; however, relatively, signal spectra of 2–3 Hz were evident. It is believed that the utilization of walking-assisted aid attachment resulted in periodicity during walking.

D. Spectrogram

The participant walked both before and after attaching the walking aid device, and spectrograms were analyzed after removing the device. Before utilizing the aid, relatively high-frequency components were observed, possibly due to instability. However, during walking without the aid, there was a reduction in relatively high-frequency components, while low-frequency components, indicative of stable walking, became predominant. Although spectrogram calculations were performed only once in this instance, making it difficult to generalize the findings, it is believed that the effectiveness of spectrograms in gait analysis has been demonstrated.

E. Gait Speed

The walking speed calculated from the slope of the step count and heel position presented in Figure 20, along with the time count from the video, indicated improvements before, during, and after the utilization of the walking aid, with speeds of 0.30 m/s, 0.36 m/s, and 0.45 m/s, respectively. This suggests that the reduction in foot instability during walking, possibly due to the utilization of the walking aid, could be one contributing factor.

V. CONCLUSIONS

The values obtained via calculation from MediaPipe, which can display skeletal certification, were compared with those of commercially available gait measurement systems to investigate the differences. The study revealed that the effects of different angles of video recording during gait should be considered in programming and in determining the results obtained with MediaPipe. However, MediaPipe can be an effective tool for determining walking conditions when the cost of implementing the system and the data required are limited.

Analysis results were obtained from assessments from PT and OT, and skeletal conditions and skeletal coordinates were obtained from media pipes regarding the walking status of participants with atherothrombotic cerebral infarction before, during, and after wearing walking aid devices. Although some results differed from the assessment because the videos were from all sides, we could obtain data that supported the PT and OT assessments in large part. By accumulating data in the future, we will be able to rehabilitate the media pipe. The application of this technology is expected to expand.

ACKNOWLEDGMENT

This work was supported by JSPS KAKENHI Grant Numbers JP20K11924 and JP23K11207. We would like to thank the patients and the staff of Seirei Yokohama Hospital their cooperation in this study.

REFERENCES

[1] Y. Uchida, T. Funayama, E. Ohkubo, and Y. Kogure, “Considerations for Applying MediaPipe to Gait Analysis,” GLOBAL HEALTH 2023, pp. 12-17, IARIA.

[2] L. G-Villanueva, S. Cagnoni, and L. Ascari, “Design of a Wearable Sensing System for Human Motion Monitoring in Physical Rehabilitation,” Sensors, vol. 13, pp. 7735-7755, 2013.

[3] Y.-L. Zheng et al., “Unobtrusive Sensing and Wearable Devices for Health Informatics,” IEEE Trans. Biomedical Engineering, vol. 61, pp. 1538-1554, 2014.

[4] M. M. Alam and E. B. Hamida, “Surveying Wearable Human Assitive Technology for the Life and Safty Critical Applocations: Standards, Challenges and Opportunities,” Sensors, pp. 9153-9209, 2014.

[5] M. J. Deen, “Information and Communications Technologies for Elderly Ubiquitous Healthcare in a Smart Home,” Personal and Ubiquitous Computing, pp. 573-599, 2015.

[6] S. Hong and K. S. Park, “ Unobtrusive Photoplethymographic Monitoring Under the Foot Sole while in a Standing Posture,” Sensors, 3239, 2018.

[7] V. Bucinskas et al., “Wearable Feet Pressure Sensor for Human Gait and Falling Diagnosis,” Sensors, 5240, 2021.

[8] P. M. Riek, A. N. Best, and R. Wu, “Validation of Inertial Sensors to Evaluate Gait Stability,” Sensors, vol. 23, 1547, 2023.

[9] T. Funayama, Y. Uchida, and Y. Kogure, “Assessment of Walking Condition Using Pressure Sensors in the Floor Mat,” The Eleventh, International Conference on Global Health Challenges, Valencia, Spain, November 15, 2022.global_health_2022_2_30_70023.

[10] T. Funayama, Y. Uchida, and Y. Kogure, “Detection of motion restriction with smart insoles,” Sensors & Transducers Journal, Vol. 259, Issue 5, pp. 61-68, 2022.

[11] S. Kim et al., “Assessing physical abilities of sarcopenia patients using gait analysis and smart insole for development of digital biomarker,”Scientific Reports, 13:10602, 2023.

[12] Y. Uchida, T. Funayama, K. Hori, M. Yuge, N. Shinozuka, and Y. Kogure, “Possibility of Detecting Changes in Health Conditions using an Improved 2D Array Sensor System,” sensors & Transuducers, Vol. 259, pp. 29-36, 2022.

[13] T. Funayama, Y. Uchida, and Y. Kogure, “Step Measurement Using a Household Floor Mat and Shoe Sensors,”, International Journal on Advances in Life Sciences, vol. 15, No. 1&2, pp. 33-43, 2023.

[14] S. Diaz, J. B. Stephenson, and M. A. Labrador, “Use of Wearable Sensor technology in Gait, Balance, and Range of Motion Analysis,” Applied Sciences, vol. 10, 234, 2020.

[15] T. Funayama, Y. Uchida, E. Ohkubo, and Y. Kogure, “Exploring the Potential of a Wrist-Worn Optical Sensor for Measuring Daily Life Activities,” GLOBAL HEALTH 2023, pp.18-24, IARIA.

[16] S. Majumder et al., “Smart Homes for Elderly Healthcare-Recent Advances and Research Challenges,” Sensors, vol. 17, 2496, 2017.

[17] K. Sato, Y. Nagashima, T. Mano, A. Iwata, and T. Toda “Quantifying normal and parkinsonian gait features from home movies: Practical application of a deep learning–based 2D pose estimator,” PLOS ONE, https://doi.org/10.1371/journal.pone.0223549, 2019.

[18] M. Windolf, N. Gotzen, and M. Morlock, “Systematic Accuracy and Precision analysis of Video motion Capturing Systems-Exemplified on The Vicon-460 system,” Journal of Biomechanics, vol. 41, pp. 2776-2780.

[19] T. B. Rodrigues, D. P. Salgado1, C. O. Cathain, N. O’Connor, and N. Murray, “Human Gait Assessment Using a 3D Marker-less Multimodal Motion Capture System,” Multimedia Tools and Applications, vol. 79, pp. 2629-2651, 2020.

[20] P. Plantard, E. Auvinet, A. S. Le Pierres, and F. Multon,”Pose Estimation with a Kinect for Ergonomic Stuidies: Evaluation of the Accuracy Using a Virtual Mannequin,” Sensors, pp. 1785-1803, 2015.

[21] R. A. Clark, B. F. Mentiplay, E. Hough, and Y. H. Pus, “Three-Dimensional Cameras and Skeleton Pose Tracking for Physical Function Assessment: A Review of Use, Validity, Current Developments and Kinect Alternatives,” Gait & Postture, vol. 68, pp. 193-200, 2019.

[22] Y. Ma, K. Mithratatne, N. Wilson, Y. Zhang, and X. Wang, “Kinect v2-Based Gait Analysis for Children with Cerebral Palsy: Validity and Reliability of Spaial Margin of Stability ad Spationtemporal Vaiables,” Sensors, vol. 21, 2104, 2021.

[23] D. Imoto, S. Hirano, M. Mukaino, E. Saitoh, and Y. Otaka, "A Novel Gait Analysis System for Detecting Abnormal Hemiparetic Gait Patterns during Robo-assisted Gait Training : A Criterion Validity Study among Healthy Adults," Frontiers in Neurorobotics, 16:1047376, 2022

[24] M. Ota, H. Tateuchi, T. Hahiguti, and N. Ichihasi, "Verification of validity of gait analysis systems during treadmill walking and running using human pose tracking algorithm," Gait and Posture, vol. 85, pp. 290-297, 2021.

[25] Y. Saiki et al., "Reliability and validity of OpenPose for measuring hip knee ankle angle in patients with knee osteoarthritis," Scientific Reports, vol. 13, 3297, 2023.

[26] V. Bazarevsky et al., "BlazePose: On-device Real-time Body Pose tracking," arXiv:2006.1204v1 [cs.CV] 2020.

[27] G. Kaur, G. Jaju, D. Agawal, K. Lyer, and C. M. Prashanth, "Implementation of Geriatric Agility Detection Using MediaPipe Pose," International Journal of Recent Advances in Multidisciplinary Topics, vol. 3, 119, 2022, ISSN:2582-7839.

[28] Y. Uchida, T. Funayama, and Y. Kogure, "Investigation of the Application of MediaPipe to Gait Analysis," GLOBAL HEALTH 2022, pp. 1-6, IARIA, 2022. ISBN: 978-1-61208-995-9.

[29] Y. Uchida, T. Funayama, and Y. Kogure, "Possibility of Gait Analysis with MediaPipe and Its Application in Evaluating the Effects of Gait-assist Devices," pp. 44-54, IARIA, International Journal on Advances in Life Sciences, vol. 15, no. 1 & 2, 2023.

[30] J.-L. Vhung, L.-Y. Ong, and M-C. Leow, "Comparative Analysis of Skelton-Based Human Pose Estimation," Future Internet, vol.14, 380, 2022.

[31] Y. Uno et al., "Validity of Spatio-Temporal Gait Parameters in Healthy Young Adults Using a Motion-Sensor-Based Gait Analysis System (ORPHE ANALYTICS) during Walking and Running," Sensors, vol. 23, 331, 2023.

[32] L. Xie et al., "TRLS: A Time Series Representation Learning Framework via Spectrogram for Medical Signal Processing," arXiv:2401.05431v1[eess.SP] 2024.